Application Note
Oct 2020
AN-850-0116

Secondary Structure Analysis of NIST Monoclonal Antibody Reference Material 8671 by Microfluidic Modulation Spectroscopy

- ○ Biosimilars
- ✓ mAbs
- ○ ADCs
- ○ AAVs
- ○ Ligand Binding
- ○ Protein/Peptide Analysis
- ○ VLPs
- ○ Nucleic Acid
- ○ Fusion Proteins
- ○ Enzyme Analysis

- ⬢ Aggregation
- ✓ Quantitiation
- ✓ Structure
- ⬢ Stability
- ✓ Similarity

www.redshiftbio.com

Introduction

In 2016 the National Institute of Standards and Technology (NIST) made NISTmAb Reference Material (RM) 8671 commercially available for the evaluation of methods used to characterize the structure of monoclonal antibodies. This then serves as a performance control against which novel processes and emerging characterization technologies could be compared. Because this mAb is so widely characterized, its evaluation using Microfluidic Modulation Spectroscopy (MMS) is an important measurement and the first step in characterizing mAbs against a reputable standard.

Relative to circular dichroism (CD) and Fourier-transform infrared spectroscopy (FTIR), Microfluidic Modulation Spectroscopy (MMS) is an emergent technology for the characterization of secondary structure with improvements in sensitivity, reproducibility, and quantitiative linearity over exisiting technologies. Since its commercial availablity in 2019, the AQS^3 pro MMS system by RedShiftBio has been adopted by several large biopharmaceutical companies for their characterization work.[1-5]

In the data presented within this note, NIST mAb RM 8671 is evaluated by MMS which proves to be a reliable and robust method for the measurement of higher order structure (HOS) across a wide concentration range.

Methods

The NIST RM 8671 IgG (lot# 3F1b) was supplied by NIST at a concentration of 100 mg/mL, along with the corresponding sample buffer of 25 mM L-Histidine at pH 6.0, The mAb stock was diluted in the matching buffer to make a dilution series of 2, 5, 10, 20, 40, 60, and 70 mg/mL. A production AQS^{3}pro MMS system was used to collect the differential absorbance spectra of each sample as it was modulated with the reference buffer through the flow cell at a rate of 1 Hz and a backing pressure of 5 psi. Spectral data was analyzed using the AQS^3 delta software Data Analysis program.

Results

I. Differential Absorbance: The differential abosorbance of the dilution series was plotted for all concentrations and is shown in Figure 1. The max DiffAU was then used to calcuate concenteration across the series.

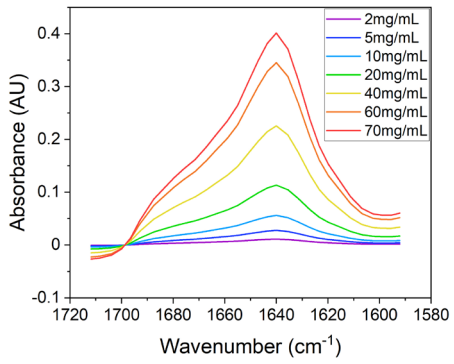

Figure 1. Differential Absorption plot for NIST mAb RM 8671 at concentrations of 2, 5, 10, 20, 40, 60, and 70 mg/mL.

REDSHIFTBio®
131 Middlesex Turnpike | Burlington, MA | 01803 | info@redshiftbio.com

Application Note
Oct 2020

Results, continued

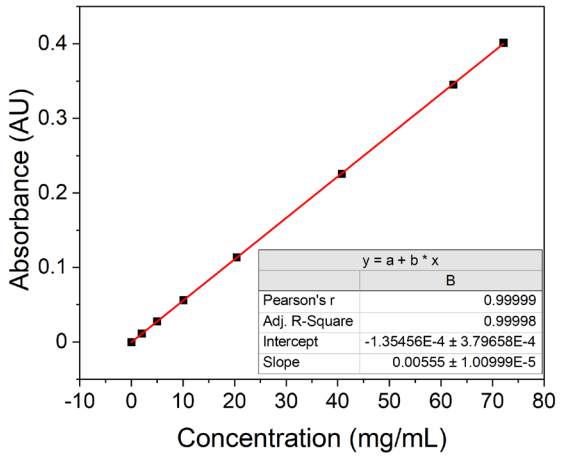

Figure 2. Quantitation plot for NIST mAb RM 8671 at all concentrations.

II. Diff AU vs Concentration: A linear plot was created from the DiffAU spectra across the concentration range as shown in Figure 2. The R-squared is exceptional with a value of >0.999. This result demonstrates the ability of the AQS³pro to quantify sample concentration over a significantly wider range than traditional technologies such as UV/Vis without sample manipulation. Table I lists the fitted concentrations relative to the nominal concentrations.

III. Absolute Absorbance: To compare secondary structure, the differential absorbance spectra are normalized for concentration to yield the absolute absorbance spectra. Figure 3 shows the absolute absorbance plot of NIST mAb RM 8671. All concentrations show excellent reproducibility in spectral overlap and peak shape.

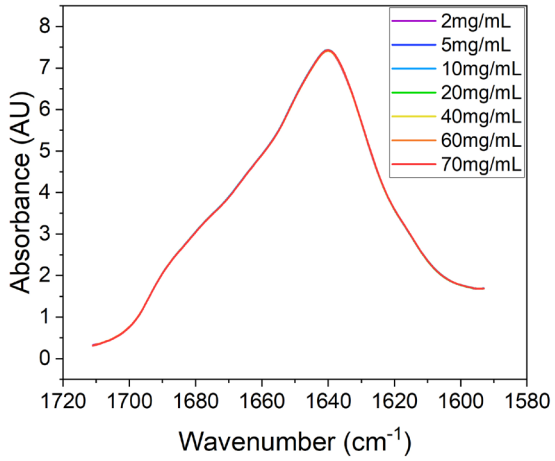

Figure 3. Absolute Absorbance plot for NIST mAb RM 8671.

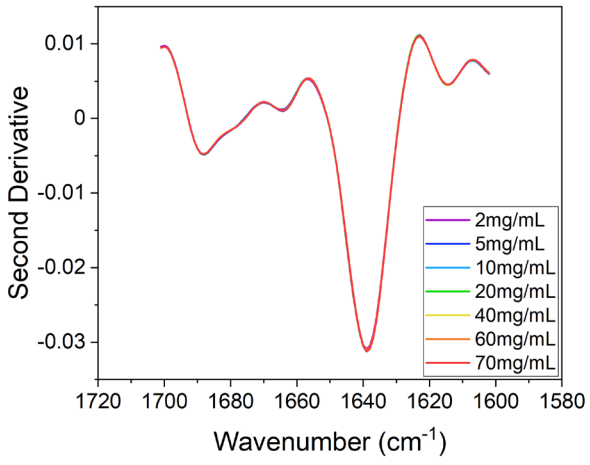

Figure 4. Second Derivative plot for NIST mAb RM 8671.

IV. Second Derivative: To better highlight slight changes in spectra, the AQS³delta software calculates the second derivative of the Absolute AU spectra. Figure 4 shows the second derivative plots of NIST mAb RM 8671 at all concentrations. The consistent overlap in second derivative spectra indicates that concentration does not impact the secondary structure of this NIST mAb over the wide experimental range.

Application Note
Oct 2020

Results, continued

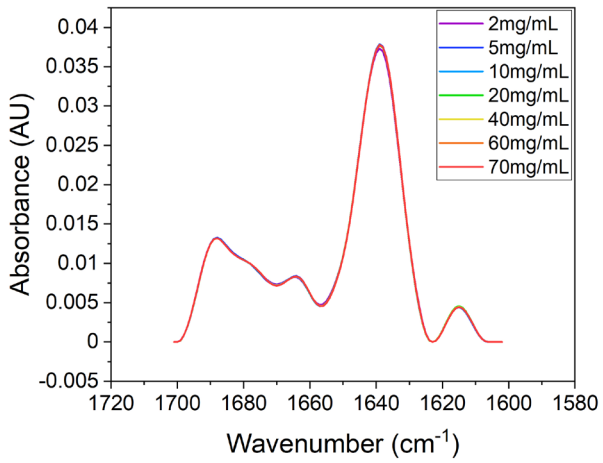

Figure 5. Area of Overlap plot for NIST mAb RM 8671.

V. Area of Overlap: To measure similarity, the AQS³delta software utilizes the inverted and baselined second derivative plot to create an Area of Overlap (AO) plot. Figure 5 shows the Area of Overlap plot for NIST mAb RM 8671 at all experimental concentrations. The Area Overlap plot was also used to calculate the similarity scores.[6] Table I shows that the NIST mAb yields similarity scores >99% across all concentrations relative to the 2 mg/mL sample. To determine if the variance is significant, the replicate variance at each concentration was compared to the replicate variance between duplicates of the 2 and 5 mg/mL samples.

Similarity calculations showed that relative to the first replicate, the second replicate similarity scores for the 2 and 5 mg/mL samples were 99.31 and 99.60% respectively. Thus, the variance in similarity between replicates is comparable to the variance in similarity calculated at all concentrations. This result highlights not only the consistency of NIST mAb, but also the high reproducibility of the AQS³pro.

Nominal Concentration (mg/mL)	Fit Concentration (mg/mL)	Similarity (%)*
2.00*	2.04	100.00
5.00	5.00	99.42
10.00	10.10	99.55
20.00	20.40	99.51
40.00	40.80	99.50
60.00	62.40	99.48
70.00	72.10	99.43

Table 1. Nominal and fitted concentrations with resulting similarity scores for NIST mAb RM 8671.

VI. Higher Order Structure: The AQS³pro calculated the HOS moities for the NIST mAb. Figure 6 shows the relative proportions of alpha-helix, beta-sheet, beta-turn, and unordered structures at all concentrations. The NIST mAb is predominantly composed of beta-sheets which is expected for antibodies.[7] The relative proportion of the various secondary structure motifs is constant across the measured concentration range. The data shows the predominant structure in this antibody is beta-sheet at 62%, followed by beta-turn at 30%, unordered structure at 7%, and alpha helix at 1%. These results are consistent with the expected proportions for typical antibody samples. Where this type of protein would be difficult to characterize using CD due to limited sensitivity for beta-sheet structures, MMS is able to resolve HOS more accurately due to non-overlapping secondary structure signals. Regarding FTIR, it is difficult to measure the relative proportions of secondary structure elements below 10 mg/mL.[3]

Application Note
Oct 2020

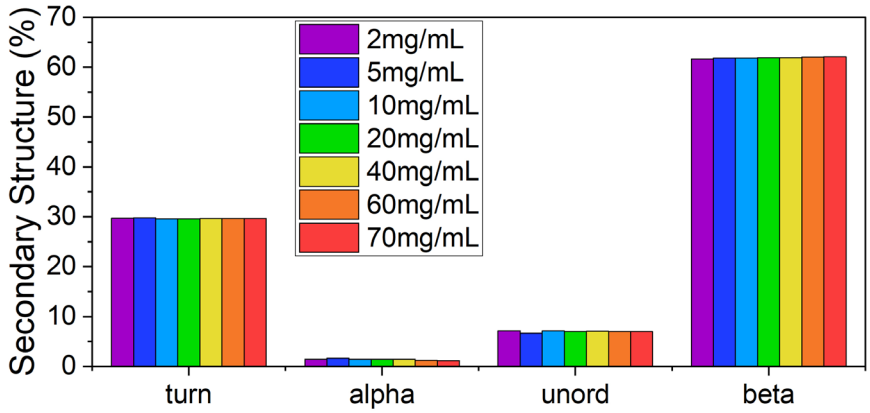

Figure 6. Higher Order Structure plot for NIST mAb RM 8671.

Conclusions

The AQS^{3}pro yielded high quality reproducible spectra over the measured concentration range of 2-70 mg/mL for NIST RM mAb 8671, and showed that it has a secondary structure composition consistent with other monoclonal antibodies - predominantly beta-sheet. This wide dynamic concentration range highlights one of the many advantages MMS provides over traditional CD and FTIR. MMS can measure samples from early stages of drug development, when sample quantity and concentrations are lower, all the way through to late stage development, where the final formulation is often more concentrated. Similarity scores of >99% at all antibody concentrations demonstrate the high sensitivity of the AQS^{3}pro, which enables it to detect the smallest changes in secondary structure. The AQS^{3}pro is therefore applicable to quality control studies for comparing lots and processing conditions throughout the development workflow.

References

1. Shea, D.; Hsu, C.-C.; Bi, T. M.; Paranjapye, N.; Childers, M. C.; Cochran, J.; Tomberlin, C. P.; Wang, L.; Paris, D.; Zonderman, J.; Varani, G.; Link, C. D.; Mullan, M.; Daggett, V. α-Sheet Secondary Structure in Amyloid β-Peptide Drives Aggregation and Toxicity in Alzheimer's Disease. PNAS 2019, 116 (18), 8895–8900. https://doi.org/10.1073/pnas.1820585116.
2. Liu, L. L.; Wang, L.; Zonderman, J.; Rouse, J. C.; Kim, H.-Y. Automated, High-Throughput Infrared Spectroscopy for Secondary Structure Analysis of Protein Biopharmaceuticals. JPharmSci 2020, 0 (0). https://doi.org/10.1016/j.xphs.2020.07.030.
3. Kendrick, B. S.; Gabrielson, J. P.; Solsberg, C. W.; Ma, E.; Wang, L. Determining Spectroscopic Quantitation Limits for Misfolded Structures. Journal of Pharmaceutical Sciences 2020, 109 (1), 933–936. https://doi.org/10.1016/j.xphs.2019.09.004.
4. Wikström, D. B. L. W. J. Z. M. Shaping IR Spectroscopy into a Powerful Tool for Biopharma Characterizations http://www.biopharminternational.com/shaping-ir-spectroscopy-powerful-tool-biopharma-characterizations-1 (accessed May 22, 2020).
5. Applications of Microfluidic Modulation Spectroscopy for Antibody-Drug Conjugate Structural Characterization http://www.americanpharmaceuticalreview.com/Featured-Articles/354821-Applications-of-Microfluidic-Modulation-Spectroscopy-for-Antibody-Drug-Conjugate-Structural-Characterization/
6. Kendrick, B. S.; Dong, A.; Dean Allison, S.; Manning, M. C.; Carpenter, J. F. Quantitation of the Area of Overlap between Second-Derivative Amide I Infrared Spectra To Determine the Structural Similarity of a Protein in Different States. Journal of Pharmaceutical Sciences 1996, 85 (2), 155–158. https://doi.org/10.1021/js950332f.
7. Dong, A.; Huang, P.; Caughey, W. S. Protein Secondary Structures in Water from Second-Derivative Amide I Infrared Spectra. Biochemistry 1990, 29 (13), 3303–3308. https://doi.org/10.1021/bi00465a022.